AUTO-SMASH: A self-calibrating technique for SMASH imaging

Peter M. Jakob [a,*], Mark A. Griswold [a], Robert R. Edelman [a], Daniel K. Sodickson [b]

[a] *Department of Radiology, Beth Israel Deaconess Medical Center, Harvard Medical School, 330 Brookline Ave, Boston, MA 02215, USA*
[b] *Department of Medicine, Cardiovascular Division, Beth Israel Deaconess Medical Center, Harvard Medical School, Boston, USA*

Abstract

Recently a new fast magnetic resonance imaging strategy, SMASH, has been described, which is based on partially parallel imaging with radiofrequency coil arrays. In this paper, an internal sensitivity calibration technique for the SMASH imaging method using self-calibration signals is described. Coil sensitivity information required for SMASH imaging is obtained during the actual scan using correlations between undersampled SMASH signal data and additionally sampled calibration signals with appropriate offsets in k-space. The advantages of this sensitivity reference method are that no extra coil array sensitivity maps have to be acquired and that it provides coil sensitivity information in areas of highly non-uniform spin-density. This auto-calibrating approach can be easily implemented with only a small sacrifice of the overall time savings afforded by SMASH imaging. The results obtained from phantom imaging experiments and from cardiac studies in nine volunteers indicate that the self-calibrating approach is an effective method to increase the potential and the flexibility of rapid imaging with SMASH. © 1998 Elsevier Science B.V. All rights reserved.

1. Introduction

One common feature of all standard fast imaging techniques is that they all acquire data in a sequential fashion. Only one portion of k-space is acquired at a time, which sets a methodological upper limit to the achievable scan time. Only a few proposals for parallel or partially parallel acquisitions (PPA) in MRI have been described in the past [1–6]. These techniques for MR scan time reduction are based on spatial encoding with multiple spatially distinct receiver coils, where each array coil is characterized by a unique spatial response, so that each receiver adds spatial information to the localization process. This information is used to reduce the number of phase encoding gradient steps. For their successful operation, all of the PPA techniques rely upon accurate knowledge or estimation of the relative RF-sensitivities of the component coils in the array used for imaging.

The SMASH technique [6], which stands for SiMultaneous Acquisition of Spatial Harmonics, is a PPA technique which extracts additional spatial information through the generation of sinusoidal spatial variations in coil sensitivity. These spatial variations, or 'spatial harmonics', take the place of spatial modulations normally produced by magnetic field gradients in conventional MR imaging which allows the simultaneous acquisition of multiple lines of MR data. It has been successfully demonstrated that SMASH can be integrated with many of the fastest existing imaging sequences, yielding multiplicative improvements in imaging speed [6]. A factor of two to three time savings has been demonstrated in vivo using SMASH with commercially available coil arrays and up to 8-fold improvements have been achieved in phantoms using specialized RF hardware [7]. In principle, there is no limit to the number of k-space lines that may be

* Corresponding author. Tel.: +1 617 6672047; fax: +1 617 6677917; e-mail: pjacob@froto.bidmc.harvard.edu

scanned simultaneously, assuming that coil arrays with sufficient numbers of independent component coils with appropriate sensitivities are available for a given field-of-view (FOV).

Although coil array based PPA imaging techniques can provide a considerable improvement in imaging speed, the greatest constraints of the PPA imaging techniques are their dependence on the accurate measurement of component coil sensitivities, since PPA reconstructions rely upon an accurate estimate of the individual coil sensitivity functions in the underlying coil array. Several strategies for coil sensitivity calibration have been proposed [5,6,8,9].

First, the coil sensitivity profiles can be calculated from the Biot–Savart law using knowledge of the coil's size, shape and position relative to the slice-of-interest (SOI). However, this approach is impractical in vivo, since the theoretical field map may correlate poorly with the actual sensitivity profiles because of unpredictable coil loading effects and inaccurate coil positioning.

Second, the sensitivity information can be obtained from images of a uniform phantom taken at the same position as the in vivo images [6,8]. This approach of an in vitro reference can be problematic in many cases, since coil loading and/or coil position may change significantly from subject to subject, thereby changing the effective coil sensitivities. In addition, acquiring and using these reference data to correct subsequent in vivo images can be impractical with flexible phased arrays, since the exact locations of the individual coils may be affected by the subject anatomy.

Third, an estimate of the coil sensitivity functions can be obtained by acquiring the required coil references in vivo in the desired image plane, an approach which was used for the first in vivo implementations of SMASH [6]. However, this approach requires that a reference image set be acquired using an appropriate imaging technique, which we term 'coil sensitivity weighted', before the post-processing of the SMASH images is possible. This procedure can be imperfect, since it requires a region of uniform spin density for a perfect calibration. In vivo this requirement is often impossible to fulfil especially in regions of highly varying spin density such as in the chest, which has very low signal-to-noise in the area of the lungs. In addition, B_0 and B_1 magnetic field inhomogeneities may distort the true coil sensitivity profiles depending on the imaging technique used. Furthermore this procedure can also be time consuming, since it has to be performed for each SOI.

Fourth, to overcome the problems mentioned above an estimate of the sensitivity profiles can be derived from a combination of body coil and array coil images of the subject [9]. In this approach, the surface coil image is divided by the body coil image to derive the array coil sensitivity profile. This approach accurately estimates the coil sensitivity functions in areas where sufficient signal-to-noise ratio is available, which may not be possible in areas such as the lungs. This method also increases scan time significantly, even when low resolution pairs of body/array coil images are acquired. In addition, this approach is difficult in moving tissue structures, since the body coil and phased array coil image have to be obtained ideally in exactly the same position. Therefore, the accuracy of this coil sensitivity calibration can be impaired in the situation of involuntary subject motion, breathing and cardiac motion. Ra and Rim [5] describe a similar method using a reference array image set without the body coil image, but otherwise suffers from the same difficulties.

In summary, PPA techniques, including SMASH, rely upon accurate estimation of the sensitivity functions of individual coils in a coil array. This can be a cumbersome, inaccurate and time-consuming procedure which in the worst case can eliminate the time advantage of PPA techniques and therefore limits potential applications of faster imaging with PPA.

In order to address these limitations, we have developed a new internal calibration technique for SMASH imaging, called AUTO-SMASH, in which coil sensitivity information can be detected during the actual scan by an auto-calibration mechanism. Details of both acquisition and reconstruction strategies in this new AUTO-SMASH approach are provided below, along with illustrative results from phantom imaging experiments. The benefits of faster imaging with SMASH may be applied to many areas of MR imaging, but the technique holds particular promise for cardiac MRI. Since the thorax has a highly inhomogeneous spin density, which renders standard sensitivity reference estimation techniques difficult, cardiac experiments are particularly well suited for the AUTO-SMASH approach. Therefore, in order to validate the proposed auto-calibration scheme and to demonstrate the benefits of imaging with AUTO-SMASH, a number of cardiac imaging experiments were performed.

2. Theory

2.1. Brief review of the SMASH technique

In order to highlight the key features of the AUTO-SMASH approach, we first summarize the basic SMASH technique by reviewing some results from Sodickson and Manning [6].

The SMASH procedure operates by using linear combinations of simultaneously acquired signals from multiple surface coils with different spatial sensitivities. These combinations are used to reconstruct missing signals in a data set with reduced phase encoding. In other words, the linear combination of component coil

signals substitutes for spatial modulations normally produced by phase encoding gradients.

In a coil array with L components, each coil l has a distinct sensitivity function $C_l(x, y)$. For a standard imaging situation, the component coil signals are combined so as to produce a composite sensitivity C_0^{comp} which extends across the region of interest:

$$C_0^{comp}(x, y) = \sum_{l=1}^{L} n_l^{(0)} C_l(x, y) \qquad (1)$$

The coil weights $n_l^{(0)}$ may be chosen, for example, to produce uniform image intensity. For such combinations, the composite MR signal for a plane with spin density $\rho(x, y)$ takes the form,

$$
\begin{aligned}
S^{comp}(k_x, k_y) &= \sum_{l=1}^{L} n_l^{(0)} S_l(k_x, k_y) \\
&= \iint dx\, dy \sum_{l=1}^{L} n_l^{(0)} C_l(x, y) \rho(x, y) \\
&\quad \exp\{-ik_x x - ik_y y\} \\
&= \iint dx\, dy\, C_0^{comp}(x, y) \rho(x, y) \\
&\quad \exp\{-ik_x x - ik_y y\} \qquad (2)
\end{aligned}
$$

where $k_x \equiv \gamma G_x t_x$ and $k_y \equiv \gamma G_y t_y$ as usual, with G_x and G_y the magnitude of the x and y gradients, and t_x and t_y the times spent in the x and y gradients respectively. Inverse Fourier-transformation of Eq. (2) with respect to k_x and k_y reconstructs the usual spin density function $\rho(x, y)$ multiplied by the composite sensitivity profile C_0^{comp}.

In the SMASH approach, signals from the various array components are combined with different linear weights, $n_l^{(m)}$, to produce sinusoidal spatial sensitivity profiles (spatial harmonics of order m) on top of the original profile C_0^{comp}:

$$
\begin{aligned}
C_m^{comp}(x, y) &= \sum_{l=1}^{L} n_l^{(m)} C_l(x, y) \\
&= C_0^{comp}\{\cos(m\Delta k_y y) + i\,\sin(m\Delta k_y y)\} \\
&= C_0^{comp} \exp(im\Delta k_y y) \qquad (3)
\end{aligned}
$$

Here m is an integer, and $\Delta k_y = 2\pi/\text{FOV}$, the minimum k-space interval corresponding to the desired FOV. The composite MR signal then becomes:

$$
\begin{aligned}
S_m^{comp}(k_x, k_y) &= \iint dx\, dy\, C_m^{comp} \rho(x, y) \\
&\quad \times \exp\{-ik_x x - ik_y y\} \\
&= \iint dx\, dy\, C_0^{comp} \rho(x, y) \\
&\quad \times \exp\{-ik_x x - i(k_y - m\Delta k_y) y\} \qquad (4)
\end{aligned}
$$

Therefore this new combination can be used to shift the measured k-space data by an amount $(-m\Delta k_y)$.

If a total of M spatial harmonics can be generated by M different linear combinations of component coil signals (including the original homogeneous combination), then M lines of k-space may be reconstructed for each application of a phase encoding gradient. Gradient based spatial phase encoding can therefore be partially replaced by an analogous spatial encoding procedure tied to the RF coil array, since the linear combination of component coil signals produces spatial modulations of precisely the same sinusoidal form as the modulations normally produced by gradients. Signal data sets may be acquired with a reduced number of phase encoding gradient steps, and the sub-encoded data from the various component coils may be combined with appropriate linear combinations to fill in the remainder of k-space required for an image with given spatial resolution and FOV. Since phase encoding gradient steps constitute the temporal bottleneck in most traditional MR imaging, the omission of all but $1/M$ gradient steps corresponds to an M-fold increase in imaging speed.

The basic procedure for SMASH reconstruction may be summarized as follows (Fig. 1(a, b)): Using knowledge of the position-dependent sensitivities of the individual coils in the RF coil array, weighted combinations of signals from each of the coils are formed to approximate the required sinusoidal modulations in sensitivity across the FOV. The appropriate composite shifted k-space signals are then formed, and the shifted data sets are interleaved, to yield the full k-space matrix. The reconstructed SMASH image is then obtained by Fourier-transformation of this matrix.

SMASH reconstructions rely upon the accurate knowledge of the RF coil sensitivity of each surface coil in the array in order to determine the optimal complex weights, $n_l^{(m)}$. In the original SMASH implementations [6], this determination was made by fitting of measured coil sensitivity data to the target spatial harmonic sensitivity profiles, using additional coil sensitivity weighted reference data sets.

2.2. AUTO-SMASH: principles

In what follows, it is shown that the set of optimal complex weights, $n_l^{(m)}$, necessary for SMASH postprocessing can also be determined using a small number of additionally recorded auto-calibration signals (ACS), which serve as a form of navigator measurement. The ACS represent lines at intermediate positions in k-space, which are phase encoded in a conventional manner using the phase encoding gradient and compared to the signals from the

SMASH acquisition. When information from these extra signals is incorporated into the reconstruction, the
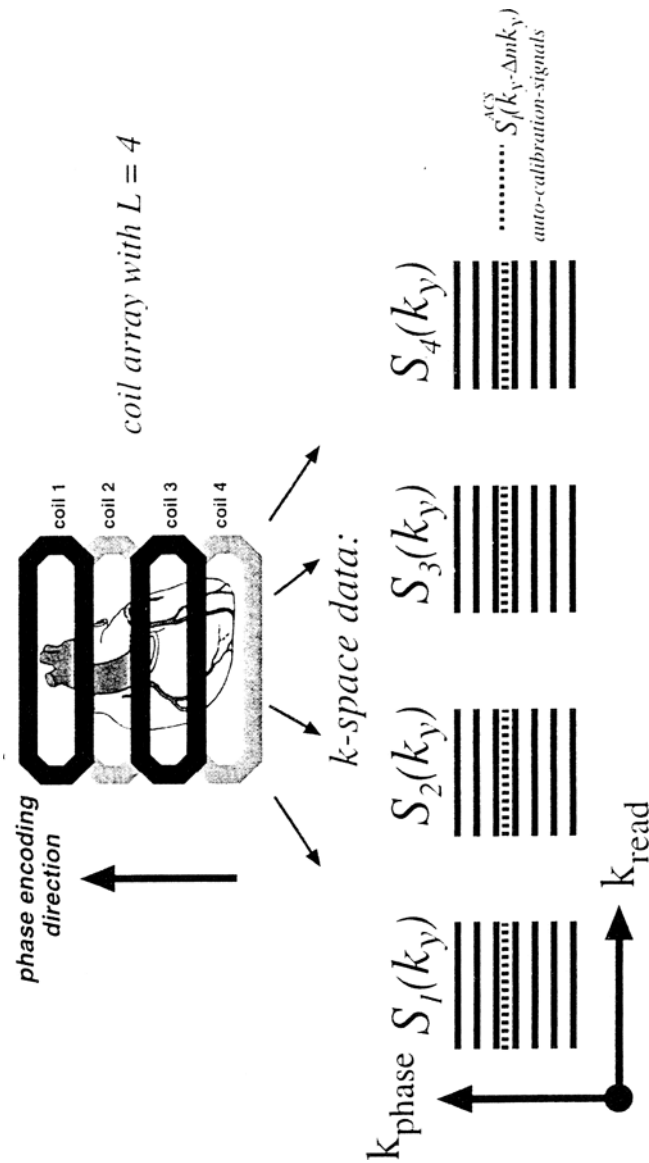
Fig. 1. Schematic representation of the SMASH/AUTO-SMASH procedure for a fourcoil cardiac phased array and $M = 2$ spatial harmonics. (a) Linear coil array with $L = 4$ coil elements and schematic k-space trajectories indicated by horizontal lines. In this representative example, every second line in k-space is sampled (solid lines). Extra sampled k-space lines, shown here as dashed lines, serve as autocalibration signals (ACS) in the AUTO-SMASH procedure. (b) The SMASH technique uses knowledge of individual coil sensitivities C_l in the linear coil array obtained from an independent coil sensitivity reference scan. Individual coil sensitivity profiles are depicted as thick solid lines beneath each component coil. Weighted combinations of these coil sensitivities are formed to approximate the required modulations in sensitivity across the FOV. The appropriate coil weightings are used here to generate two linear combinations (0th and 1st spatial harmonic). Combined coil sensitivity profiles are indicated by solid lines. (c) The AUTO-SMASH technique uses additionally sampled ACS signals $S_l^{ACS}(k_x, k_y - m\Delta k_y)$, represented by dashed echoes (bottom). From these signals a composite reference line $S^{comp}(k_x, k_y - m\Delta k_y)$ is formed and is presented as a single solid echo. Afterwards this composite signal $S^{comp}(k_x, k_y - m\Delta k_y)$is used as a target for fitting of the four coil signals $S_l(k_x, k_y)$ which are also represented as solid echoes (top). This fitting procedure yields the optimal coil-weighting factors $n_l^{(m)}$ necessary for the final SMASH reconstruction. This procedure does not require the intermediate of spatial harmonic generation and the effect is the same as if coil sensitivities had been fitted to spatial harmonic target profiles.

c   AUTO-SMASH

$S_l(k_y)$

$n_l^{(0)}$

0-th. harmonic generation

$$\sum_{l=1}^{L} n_l^{(0)} S_l(k_x, k_y) = S^{comp}(k_x, k_y)$$

$n_l^{(m)}$

m-th. harmonic generation

$$\sum_{l=1}^{L} n_l^{(m)} S_l(k_x, k_y - m\Delta k_y) = S^{comp}(k_x, k_y - m\Delta k_y)$$

$n_l^{(0)}$

$$\sum_{l=1}^{L} n_l^{(0)} S_l^{ACS}(k_x, k_y - m\Delta k_y) = S^{comp}(k_x, k_y - m\Delta k_y)$$

Auto-calibration-signals $S_l^{ACS}(k_x, k_y - m\Delta k_y)$

b   SMASH

C_1 C_2 C_3 C_4

coil sensitivity functions $C_l(x,y)$

phase encoding direction

$n_l^{(0)}$

0-th. harmonic generation

real

imaginary

$$\sum_{l=1}^{L} n_l^{(0)} C_l(x,y) = 1$$

$n_l^{(m)}$

m-th. harmonic generation

real

imaginary

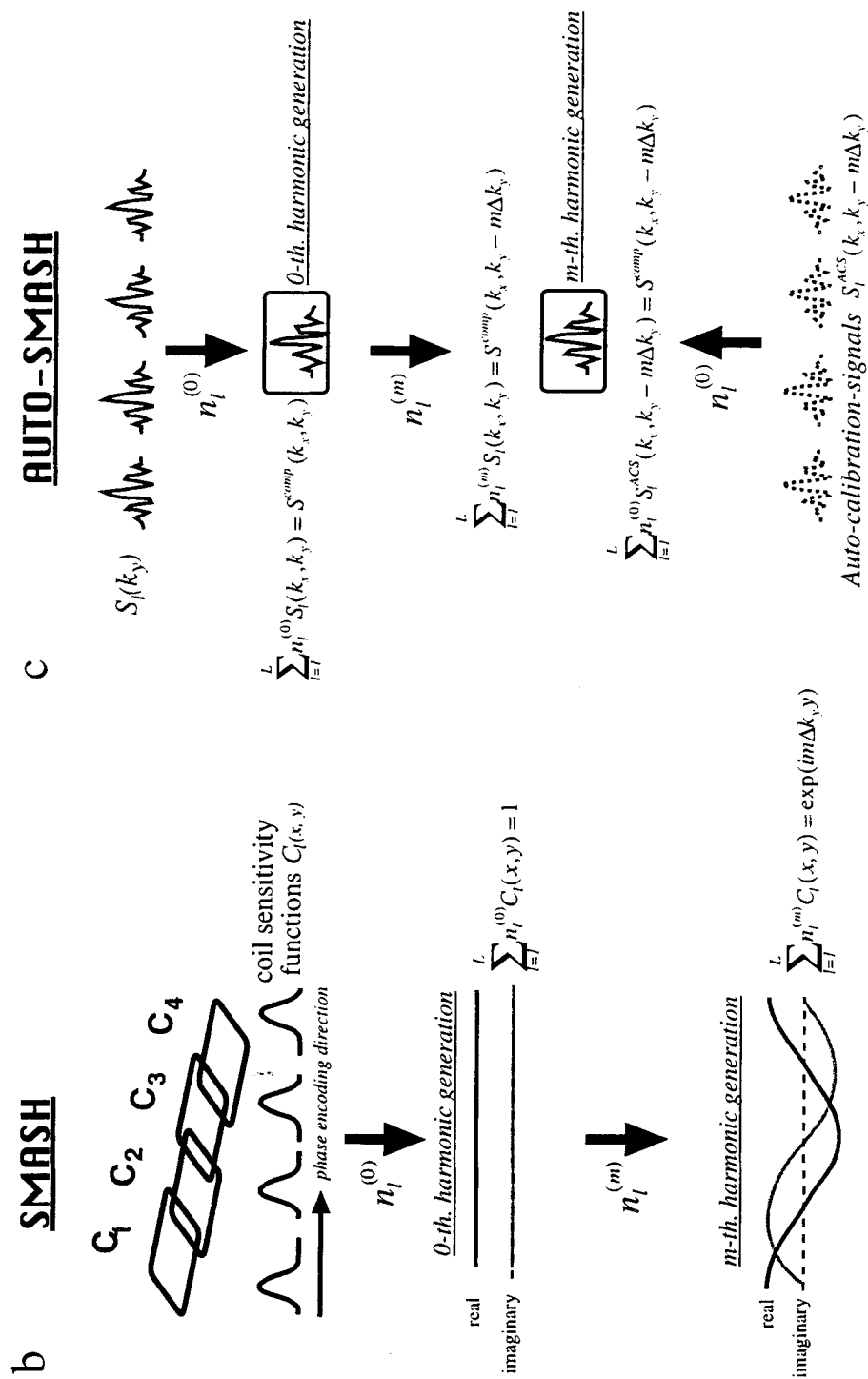$$\sum_{l=1}^{L} n_l^{(m)} C_l(x,y) = \exp(im\Delta k_y y)$$

Fig. 1. (Continued)

set of linear weights, $n_l^{(m)}$, may be extracted automatically for each acquisition without the intermediate step of coil sensitivity measurements. This auto-calibrating approach can be easily implemented with only a small sacrifice of the overall time savings afforded by SMASH imaging.

In SMASH, linear combinations of component coil signals are used to generate composite signals shifted by an amount ($-m\Delta k_y$) in k-space. In AUTO-SMASH a few extra navigator ACS-lines are acquired during the actual scan which are exactly shifted by the same amount($-m\Delta k_y$). Relations between the SMASH data set and these extra ACS-data may then be used to extract the desired optimal complex weights, $n_l^{(m)}$, as follows.

First consider the composite signal generated by uniform combination of component coil signals $S_l^{ACS}(k_x, k_y - m\Delta k_y)$ at position $(k_y - m\Delta k_y)$ in k-space:

$$S^{comp}(k_x, k_y - m\Delta k_y) = \sum_{l=1}^{L} n_l^{(0)} S_l^{ACS}(k_x, k_y - m\Delta k_y)$$

$$= \int\int dx\, dy \sum_{l=1}^{L} n_l^{(0)} C_l(x, y)\rho(x, y)$$

$$\exp\{-ik_x x - i(k_y - m\Delta k_y)y\} \quad (5)$$

Alternatively, as outlined in the previous section, the same composite signal may be formed by appropriate combinations of signals $S_l(k_x, k_y)$ at position k_y in k-space, through generation of a spatial harmonic of order m which has already been shown to produce a k-space shift of $-m\Delta k_y$.

$$S^{comp}(k_x, k_y - m\Delta k_y) = \sum_{l=1}^{L} n_l^{(m)} S_l(k_x, k_y)$$

$$= \int\int dx\, dy \sum_{l=1}^{L} n_l^{(m)} C_l(x, y)\rho(x, y)$$

$$\exp - ik_x x - ik_y y\} \quad (6)$$

A simple comparison of Eq. (5) with Eq. (6) yields

$$\sum_{l=1}^{L} n_l^{(m)} S_l(k_x, k_y) = \sum_{l=1}^{L} n_l^{(m)} S_l^{ACS}(k_x, k_y - m\Delta k_y) \quad (7)$$

Therefore, if extra k-space lines $S_l^{ACS}(k_x, k_y - m\Delta k_y)$ are acquired as auto-calibration signals during a SMASH acquisition, a composite reference line $S^{comp}(k_x, k_y - m\Delta k_y)$ may be formed from these signals. The SMASH lines $S_l(k_x, k_y)$ may then be fitted directly to the reference line $S^{comp}(k_x, k_y - m\Delta k_y)$ without requiring the intermediate of spatial harmonic generation. The effect is the same as if coil sensitivities had been fitted to spatial harmonic target profiles. Similar weights $n_l^{(m)}$ are produced, since the relation between different lines of k-space remains a relation of spatial

harmonics. After fitting, these same weights $n_l^{(m)}$ may be used to form the required signal combinations in a SMASH reconstruction. Fig. 1(c) is a pictorial summary of stages in a practical AUTO-SMASH imaging procedure, shown for comparison next to the correponding procedure in the original SMASH technique.

In general for AUTO-SMASH, the pulse sequence and gradient phase encoding tables have to be modified, so that for every desired spatial harmonic function m, an additional signal $S_l^{ACS}(k_x, k_y - m\Delta k_y)$ is acquired along the $k_y - m\Delta k_y$ line in k-space during the actual scan. Thus, for every spatial harmonic, an auto-calibration line of data is acquired, which adds only $(M - 1)T$ to the SMASH scan time, where T represents the repetition time or inter-echo spacing of the applied imaging technique.

In summary, the AUTO-SMASH self calibration procedure replaces an experimentally cumbersome and potentially inaccurate coil sensitivity measurement with a targeted acquisition of a few extra lines of MR signal data. The underlying spatial harmonic modulations produced by phase encoding gradients in these extra data lines are used to 'train' the linear combinations required for SMASH reconstruction. Since it is the relations between MR signals rather than the absolute coil sensitivities which are used for determination of optimal signal weightings, the effects of spin density variations are largely eliminated and AUTO-SMASH may be used even in regions of markedly inhomogeneous spin density. A flowchart of the AUTO-SMASH procedure is shown in Fig. 2.
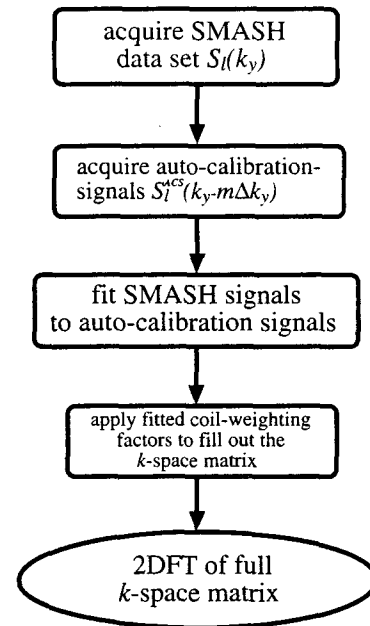

Fig. 2. A flow chart summarizing the major steps in the AUTO-SMASH procedure.

3. Methods

All raw data were generated on a Siemens Vision 1.5 T whole body clinical MR scanner (Siemens, Erlangen, Germany). The system has a resonant EPI capability with minimum gradient rise time of 300 μs or non-resonant rise time of 600 μs to a peak gradient amplitude of 25 mT m^{-1} along all three axes. A prototype cardiac coil array with four overlapped component coils, with a total spatial extent of 260 mm in the phase encoding direction and 230 mm in the read direction, was used for all cardiac scans. The array extends in the head-foot direction and was used in a receive only mode with the body coil providing homogeneous excitation. During transmit, the array was actively decoupled from the body coil. The individual coil data were exported to a Hewlett–Packard 735 UNIX workstation for postprocessing. Fitting of the coil weighting functions and image reconstruction were performed in the Matlab programming environment (The Mathworks, Natick, MA).

3.1. Phantom images

In order to assess the performance of the AUTO-SMASH approach in a well-controlled experiment, a resolution phantom was imaged using the 4-element array. Images were acquired in an 8 mm thick coronal slice parallel to and approximately 60 mm above the plane of the array. A FLASH imaging sequence was used, with TE = 6 ms, TR = 12 ms, and flip angle = 15°. Phase encoding was performed in the direction of the array. FOV was 320 × 320 mm and matrix size was 128 × 128 for the full-time reference images. Reduced-time data sets with two or three times the phase encode step and hence one-half or one-third the FOV and matrix size in the phase encode direction were used for SMASH and AUTO-SMASH reconstructions. Reference component coil images were combined using a conventional sum of squares algorithm. SMASH reconstructions used coil sensitivity information taken from intensity profiles across the center of the full FOV component coil reference images to fit two or three spatial harmonics, as described above and in Sodickson and Manning [6]. AUTO-SMASH reconstructions used additionally acquired auto-calibration signals with appropriate offsets corresponding to the first and second spatial harmonics to determine component coil weight factors. In order to test the robustness of the AUTO-SMASH fitting procedure, either high signal-to-noise ratio (SNR) echoes in the center of k-space or low SNR echoes from the edge of k-space were used in alternative AUTO-SMASH reconstructions. It should be noted that the choice of reference weights $n_l^{(0)}$ for SMASH or AUTO-SMASH reconstructions is arbitrary, however that choice will be reflected in the overall intensity profile of the reconstructed image. For the phantom images presented here, reference weights yielding the most homogeneous intensity profile possible (i.e. approximately a flat zeroth spatial harmonic) were used.

3.2. Cardiac images

Since SMASH effectively allows multiple acquisitions to proceed simultaneously, it may be used to gather high resolution information in a given acquisition time, or else to acquire images of a given spatial resolution in a shorter acquisition time. Thus, the SMASH technique, when supplemented with AUTO-SMASH calibration, offers a possible remedy for the competing constraints of spatial versus temporal resolution in cardiac MRI. In this study two different acquisition strategies were implemented in order to demonstrate the benefits of AUTO-SMASH for cardiac imaging:

I. Since a reduction in breath-hold times is particularly important for patients with cardiac disease for whom current long breath-hold times are impractical, the AUTO-SMASH strategy was used to reduce breath-hold durations by a factor of 2 to 3 while maintaining constant spatial resolution.

II. Alternatively, the breath-hold time was held constant, and AUTO-SMASH was used to double the spatial resolution in the phase encoding direction (in combination with a doubled resolution in the read-out direction). This strategy results in an increased spatial resolution for a given breath-hold time.

Nine healthy volunteers (two females, seven males; age range 21–64 years) were examined according to the guidelines of the internal review board of the Beth Israel Deaconess Medical Center. Informed consent was obtained before each study. For all the studies presented here, cardiac AUTO-SMASH images with two and three harmonics ($M = 2$ and 3) were acquired using a segmented turbo FLASH sequence. The segmented turbo FLASH sequence was used for all our cardiac SMASH studies, since it is a widely used clinical technique for cardiac imaging and is easy to combine with the SMASH approach.

The following imaging protocols for strategy I and II were used:

For strategy I sequences with nine or five k-space lines per segment were used:

● Segmented turbo FLASH with 9 lines per segment: flow compensation in slice and read direction, incremented flip angle series (18, 20, 22, 25, 31, 33, 38, 48, and 90°). A TR of 14.4 ms and a TE of 7.3 ms resulted in an effective temporal resolution of 131 ms. The image matrix was 144 × 256 (reference) or 72 × 256 (AUTO-SMASH, reconstructed to 144 × 256).

- Segmented turbo FLASH with five lines per segment: flow compensation in slice and read direction, constant flip angles between 30 and 40°. A TR of 11.8 ms and TE of 6.1 ms resulted in an effective temporal resolution of 59 ms. Image matrix was 240 × 256 (reference) or 80 × 256 (AUTO-SMASH, reconstructed to 240 × 256).

For strategy II segmented turbo FLASH sequences with 9 lines per segment and an image matrix of 144 × 256 (reference) or 144 × 512 (AUTO-SMASH, reconstructed to 288 × 512) were used.

For coronary imaging a chemical shift selective fat-saturation pulse was applied before each segment to null the signal from epicardial fat and thus enhance the contrast of coronary blood flow. The data were acquired in 5–9 mm thick slices, either in a coronal orientation or in an oblique plane extending from the coronal to the sagittal direction. Prospective ECG-gating was used to place the acquisition of each segment in mid diastole. All images were obtained during a single end-expiratory breathhold with the subjects in a prone position above the coil array.

As in the phantom experiment, reference images were combined using a sum of squares algorithm. Since in vivo sensitivity references were not readily available due to the marked variation in spin density across the thorax, AUTO-SMASH was used to obtain component coil weighting factors. In all cases, a reduced data set plus one or two extra ACS lines with appropriate offsets corresponding to the first and the second spatial harmonics were acquired.

For the in vivo implementation, only high SNR echoes in the center of k-space were used as ACS. For convenience, uniform reference weights $n_l^{(0)} = 1$ were used for the in vivo images, which still corresponded to roughly homogeneous overall intensity profiles.

4. Results

As a verification of the basic relation expressed in Eq. (7), Fig. 3 shows a comparison of composite signals formed from the ACS data with composite SMASH signals after the fitting procedure depicted in Fig. 1(c). Fig. 3(a) shows the composite signal $S^{comp}(k_x, k_y - m\Delta k_y)$ formed by uniform combination of the ACS signals of the four coils in the array (left before and right after Fourier-transformation). This composite ACS was used as a target for spatial harmonic fitting of the signals $S_l(k_x, ky)$. The results of the fit are shown in Fig. 3(b) (left before and right after Fourier-transformation) and demonstrate a good correlation with the target function.

Fig. 4 shows results obtained from the phantom experiment, using two (left hand column) and three
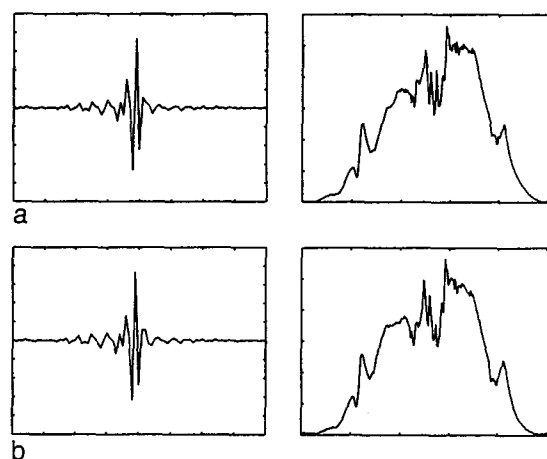

Fig. 3. Comparison of composite signals formed from the ACS data with composite SMASH signals in an actual AUTO-SMASH implementation. (a) Composite signal $S^{comp}(k_x, k_y - m\Delta k_y)$ formed by uniform combination of the ACS signals of the four coils in the array (left before and right after Fourier-transformation). This composite ACS-signal was used as a target for spatial harmonic fitting of the signals $S_l(k_x, k_y)$. (b) Composite SMASH signals after fitting (left before and right after Fourier-transformation).

(right hand column) spatial harmonics. The top row shows the full time reference images. The second row shows the reconstructed half/third time SMASH images. The SMASH images were reconstructed using coil sensitivity information obtained from a vertical intensity profile across the component coil reference images of the phantom. The third row shows the corresponding half/third time images after AUTO-SMASH reconstruction using high SNR echoes in the center of k-space as ACS. The fourth row shows the half/third time images after AUTO-SMASH reconstruction using low SNR k-space echoes from the edge of k-space as ACS. Finally, the bottom row shows AUTO-SMASH images which were reconstructed using deliberately mistuned coil-weighting factors (the weighting factors for second and third spatial harmonics were arbitrarily chosen to be replicas of the zeroth harmonic reference weights). These inappropriate weights were used in order to demonstrate the nature of image artifacts which arise when no effort is made to obtain correct coil weighting information from the ACS. Table 1 contains the fitted coil weighting factors obtained in the case of two spatial harmonics for each of the SMASH or AUTO-SMASH reconstruction strategies shown in Fig. 4.

The images in Figs. 5–7 demonstrate in vivo results obtained with the AUTO-SMASH technique with two to three spatial harmonics and a nearly twofold or threefold increase in acquisition speed.

The images in Fig. 5 are results obtained from a coronary imaging study with strategy I and II using two spatial harmonics. This data set was acquired in an 8 mm thick coronal slice parallel to and approximately
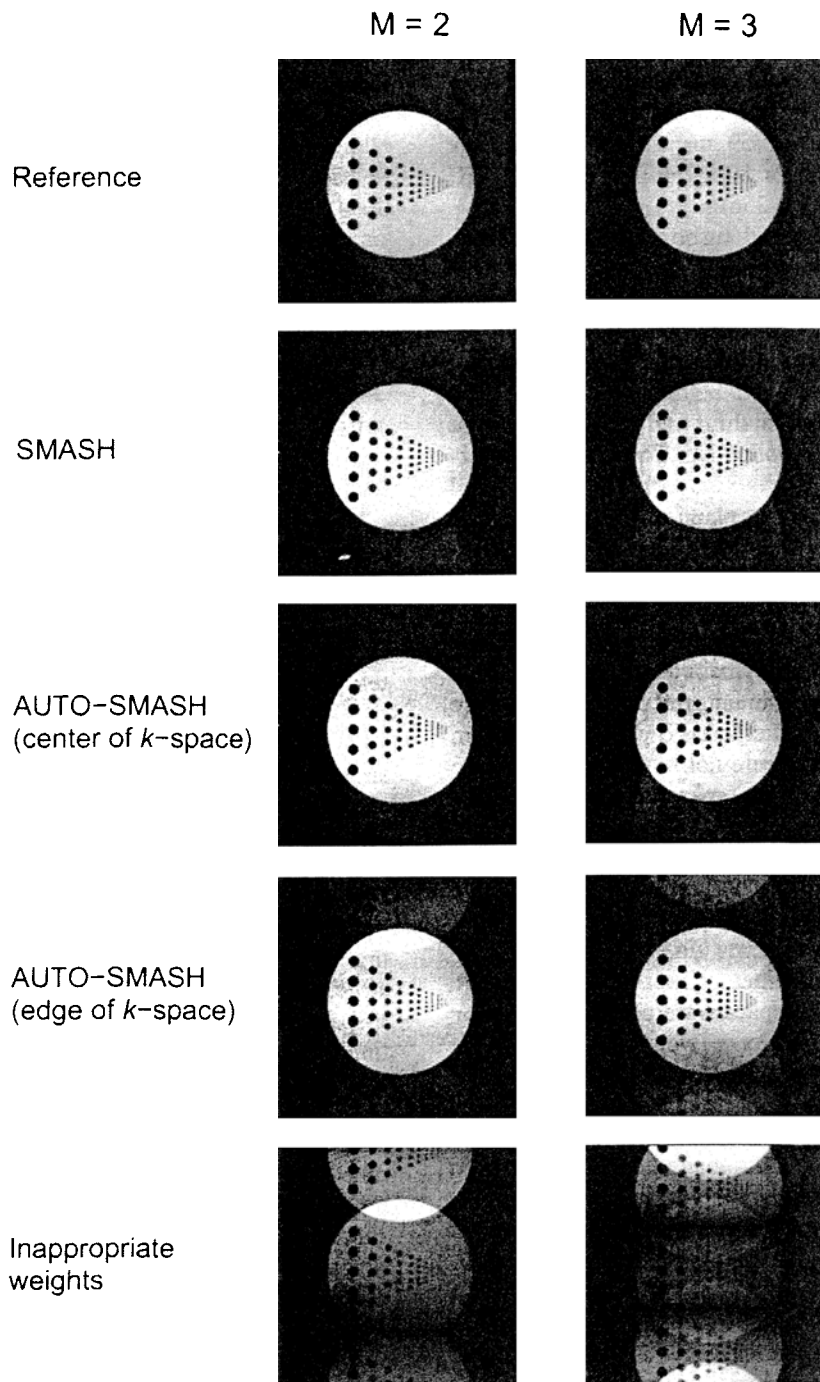
M = 2   M = 3

Fig. 4. Imaging results from a phantom study using various SMASH and AUTO-SMASH reconstructions. Left hand column: acceleration factor $M = 2$, right hand colum: acceleration factor $M = 3$. Top row: Full time reference images. Second row: Reconstructed half/third time SMASH images. Third row: Corresponding half/third time images after AUTO-SMASH reconstruction using high SNR echoes in the center of k-space as ACS. Fourth row: Half/third time images after AUTO-SMASH reconstruction using low SNR echoes from the edge of k-space as ACS. Bottom row: Images reconstructed using inappropriate coil-weighting factors (second and third harmonic weights chosen to be simple replicas of the zeroth harmonic weights).

50 mm above the plane of the cardiac array. Fig. 5(a) shows as a reference the full time (16 cardiac cycles) image with a 144×256 matrix size. Fig. 5(b) shows the corresponding half time (eight cardiac cycles) im-

age obtained with strategy I with a 144×256 matrix size after AUTO-SMASH reconstruction. The image quality is preserved in the accelerated AUTO-SMASH image. Fig. 5(c) shows the corresponding double

Table 1

Coil weighting factors used for SMASH/AUTO-SMASH reconstructions with two spatial harmonics displayed in Fig. 4, left column

	Coil 1	coil 2	Coil 3	Coil 4
SMASH	$0.270 - 1.198i$	$-0.036 - 1.765i$	$-0.256 + 0.408i$	$-0.256 + 1.400i$
AUTO-SMASH (center of k-space)	$0.124 - 1.330i$	$-0.060 - 1.317i$	$-0.513 + 0.451i$	$-0.227 + 1.221i$
AUTO-SMASH (edge of k-space)	$-0.471 - 0.771i$	$1.292 + 0.326i$	$1.221 - 0.079i$	$0.154 + 0.940i$
Inappropiate weights	$0.328 - 0.776i$	$0.489 + 0.048i$	$-0.573 - 1.328i$	$-0.129 - 1.472i$

resolution image obtained with strategy II in the same total acquisition time as the reference image. Matrix size in this image was 288×512 after AUTO-SMASH reconstruction. Details from Fig. 5(a and c) are shown in Fig. 5(d and e), respectively. A long segment of the right coronary artery may be seen running vertically near the mid-line in both these images (black arrows), but is significantly sharper in the high-resolution AUTO-SMASH image. Branches of the left coronary system (thick white arrow) may also be discerned in the AUTO-SMASH image, whereas they are not seen in the reference image. Finally, internal mammary arteries, invisible in the reference image, may be discerned running down the center of the AUTO-SMASH image (thin white arrow). The visibility of the internal mammary arteries along with the anterior heart surface in this slice results from the 8 mm slice thickness, the prone positioning of the subject (which brings the heart forward), and the anterior position of the coronal slice.

Fig. 6 presents two additional cardiac data sets. The oblique slices extending from the coronal to the sagittal direction were obtained in a healthy subject with strategy I and II using two spatial harmonics. Fig. 6(a and d) show as a reference the full time (16 cardiac cycles) images (144×256 matrix size). Fig. 6(b and e) show the corresponding half time (eight cardiac cycles) strategy I AUTO-SMASH images (144×256 matrix size). Again the image quality is preserved in the accelerated AUTO-SMASH images. Fig. 6(c and f) show the corresponding double resolution strategy II AUTO-SMASH images (288×512 matrix size) obtained in the same time as the reference images. In the oblique images shown in Fig. 6(d–f), the left main coronary artery may be seen near its origin. This image data set demonstrates that the AUTO-SMASH reconstruction is robust enough to accommodate a certain degree of image plane angulation. Note that the AUTO-SMASH reconstructions are almost entirely free of foldover artifacts. These cardiac examples confirm that AUTO-SMASH allows for an accurate calibration in regions of highly non-uniform spin density, where no reliable in vivo sensitivity reference map could be obtained.

Finally, Fig. 7 shows results obtained from a cardiac study with strategy I, in this case using three spatial harmonics. Fig. 7(b) shows the third time aliased image (80×256 matrix size), which was formed by combining

the component coil images pixel-by-pixel as the square root of the sum of square magnitudes. Fig. 7(c) right shows the corresponding third time image after AUTO-SMASH reconstruction (240×256 matrix size). This corresponds to a threefold reduction in breathhold-time. For image comparison a reference image shown in Fig. 7(a) was obtained in 48 cardiac cycles corresponding to a breath-hold time of 40 s. Even though there are some residual foldover and ghosting artifacts visible in the AUTO-SMASH reconstruction, the heart and the left coronary artery are still well depicted in the accelerated AUTO-SMASH image.

5. Discussion

One notable constraint of the original SMASH imaging technique is its dependence on the measurement of component coil sensitivities for spatial harmonic generation. AUTO-SMASH is a flexible tool for internal sensitivity reference estimation. It has the major advantage that optimal component coil weights can be determined for each individual scan independently and without a significant increase in imaging time.

However, AUTO-SMASH, like SMASH, presumes that the coil encoding procedure provided by the underlying coil array matches the conditions of Fourier-encoding or in other words that the necessary spatial harmonics may be faithfully represented by linear superpositions of component coil sensitivities. In cases for which the combined sensitivities deviate from ideal spatial harmonics, reconstruction artifacts are visible in both SMASH and AUTO-SMASH image reconstructions. The phantom images of Fig. 4 illustrate the appearance of $N/2$ and $N/3$ ghosts for the $M = 2$ and 3 reconstructions with various degrees of imperfection in the component coil weights. Similar artifacts may be seen in the in vivo $M = 3$ AUTO-SMASH reconstruction in Fig. 7, and these artifacts are responsible for much of the apparent degradation in image quality. Thus, just as in the original SMASH procedure, any errors in spatial harmonic generation will lead to image artifacts which cannot be removed by the AUTO-SMASH approach. In general, AUTO-SMASH shares the same operating limits as SMASH. The geometry of the underlying coil array will place certain limitations
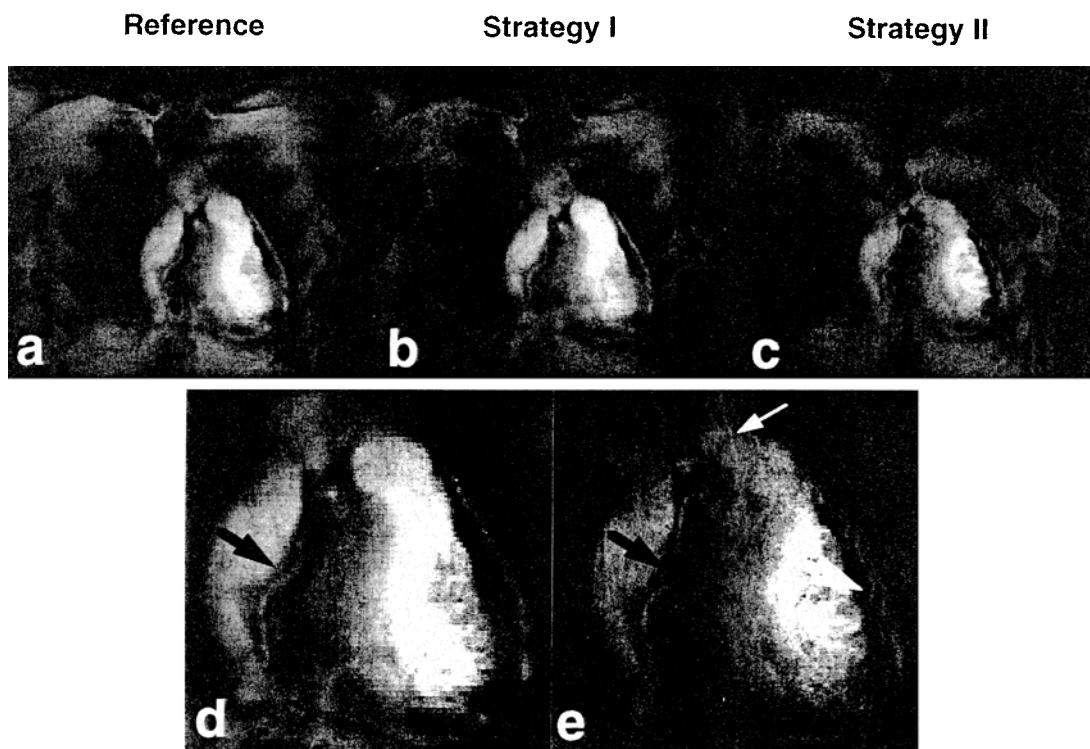
Reference   **Strategy I**   **Strategy II**

Fig. 5. Coronary imaging with AUTO-SMASH (a) Reference image (144 × 256 matrix size) obtained in 16 cardiac cycles. (b) The corresponding image obtained with strategy I in eight cardiac cycles with 144 × 256 matrix size after AUTOSMASH reconstruction. (c) Double resolution image obtained with strategy II in 16 cardiac cycles with a 288 × 512 matrix size after AUTO-SMASH reconstruction. (d, e) Details from (a) and (b) and (c), respectively. A long segment of the right coronary artery may be seen running vertically near the mid-line in these images (black arrows). Branches of the left coronary system (thick white arrow) may also be discerned in the AUTO-SMASH image, whereas they are not seen in the reference image. Finally, internal mammary arteries, invisible in the reference image, may just be discerned running down the center of the AUTO-SMASH image (thin white arrow).

on the FOV, the position across the subject, and the angulation of planes suitable for the SMASH/AUTO-SMASH reconstruction. PPA techniques, including SMASH and AUTO-SMASH, rely upon accurate matching of the sensitivity functions of individual coils in a coil array with a given FOV. Therefore, future work must involve the design of tailored RF coil arrays for AUTO-SMASH, which will allow accurate and flexible spatial harmonic generation over appropriate fields-of-view.

As demonstrated in the phantom study, component coil weights produced by SMASH and AUTO-SMASH are similar but not exactly the same. Just as in the coil-sensitivity fitting procedure used in SMASH, the accuracy of the self-calibration approach is affected by noise, which is demonstrated in Fig. 4, where the results of reconstructions using ACS from the center and the edge of k-space were compared. ACS from the edge of k-space with higher noise levels produce significantly different coil-weighting factors, though viable reconstructions with only a partial increase in aliasing artifacts were still produced (The quality of AUTO-SMASH reconstructions using these uniformly low SNR calibration signals is also indicative of what may be expected

for situations in which one or more component coils have comparatively low signal). By contrast, the deliberately mis-tuned weights produced markedly aliased images in Fig. 4. These results give a sense of the degree of robustness of the AUTO-SMASH fitting procedure.

In our current in vivo implementations, only high signal-to-noise k-space lines were used as ACS. In general, it would also be possible to use several ACS lines for each harmonic in order to improve the determination of the optimal coil weights and the accuracy of the image reconstruction. Alternatively, one extra ACS could be acquired after switching the read and the phase encoding directions. The result of such an acquisition would be an ACS data line spanning many spatial harmonics. The relations between many different harmonics k_y and $k_y - m\Delta k_y$ could then be derived from this single ACS line. In general a variety of different acquisition strategies is possible. Future studies will address the optimum postprocessing procedure in the presence of noise.

The timing of AUTO-SMASH acquisitions may also vary. The extra ACS may be acquired before, during, or immediately after the actual scan, or else in an independent scan.

Reference   **Strategy I**   **Strategy II**
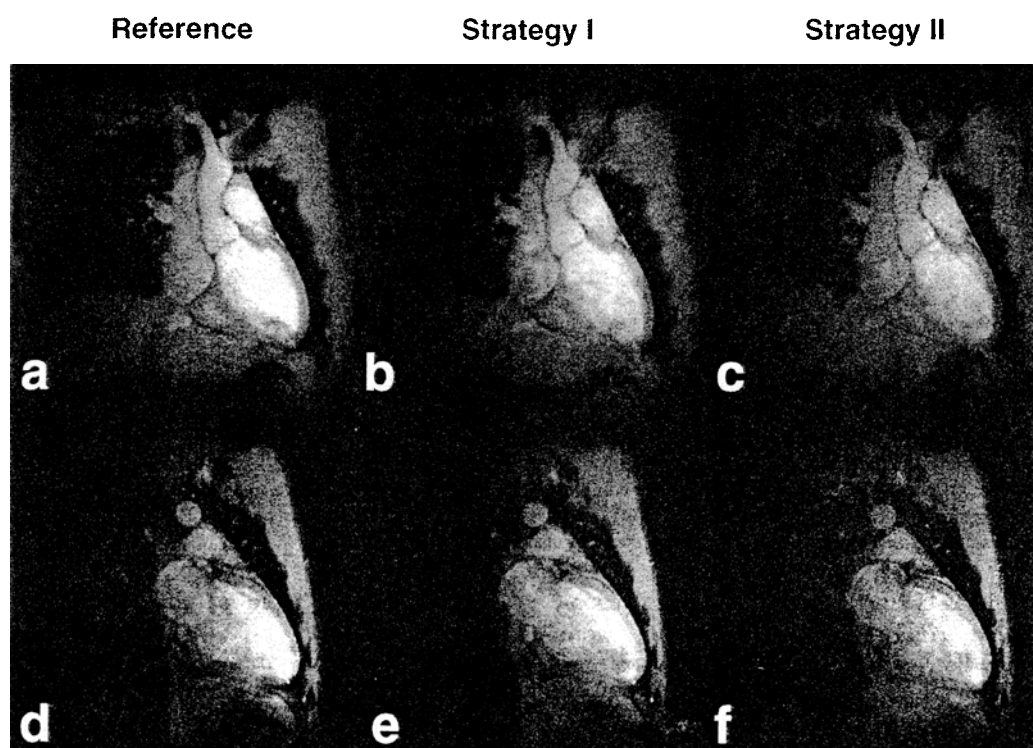

Fig. 6. Cardiac imaging with AUTO-SMASH. Oblique slices obtained in a healthy volunteer with strategy I and II and two spatial harmonics. (a, d) Full time reference images obtained in 16 cardiac cycles with 144 × 256 matrix size. (b, e) The corresponding half time images obtained with strategy I in eight cardiac cycles with 144 × 256 matrix size after AUTO-SMASH reconstruction. (c) The corresponding double resolution i;nages obtained with strategy II in 16 cardiac cycles with 288 × 512 matrix size after AUTO-SMASH reconstruction

Although we have so far described AUTO-SMASH in terms of extracting necessary coil sensitivity information, it may also be viewed in another way. Rather than simply producing ideal spatial harmonics, using combinations of component coil sensitivities, AUTO-SMASH reproduces as accurately as possible the actual effects of the experimentally applied phase encoding gradients. Each fit to an ACS target line constitutes an approximation of the actual gradient profiles, including any nonlinearities or other imperfections which may be present in these profiles. Thus, each fit acts as an effective gradient set similar in structure to the physically applied gradients. Reconstruction artifacts, when they occur, will result from mismatch between these effective gradient sets.

In this study of healthy volunteers, diagnostic images of the heart and the coronary arteries were consistently produced and clearly demonstrate the potential of the AUTO-SMASH technique for cardiac imaging and MR coronary angiography. As expected, the AUTO-SMASH images obtained with strategy II showed improved spatial resolution. For fine structures predominantly oriented parallel to the phase encoding direction, such as the right coronary artery in Fig. 5(e), some of the apparent improvement results from higher read-direction resolution. However, for structures such

as the left main coronary artery shown in Fig. 6(f) running almost parallel to the read-direction, improved visibility is predominantly a result of the increased spatial resolution in the phase encode direction. One consequence of the higher spatial resolution in strategy II is a reduced SNR, as may be appreciated in the images of Figs. 5 and 6. In addition, factors involving the component coil weightings affect SNR in SMASH and AUTO-SMASH reconstructed images. Reconstruction-related SNR considerations are the same in AUTO-SMASH as in SMASH, and these are treated in detail elsewhere [10,11].

Cardiac AUTO-SMASH, as evaluated in this study, has one important limitation: The need to acquire images nearly parallel to the underlying linear phased array coil. Since multiple image plane orientations are commonly used in cardiac imaging, careful engineering of shaped coil arrays with an increased number of array elements and optimization of postprocessing algorithms are called for in order to maintain full flexibility for routine cardiac MR applications.

The results presented in this report show the potential advantages of the AUTO-SMASH approach. It can provide important information about coil sensitivities even in areas of inhomogeneous spin density, which would otherwise render in vivo coil sensitivity mapping
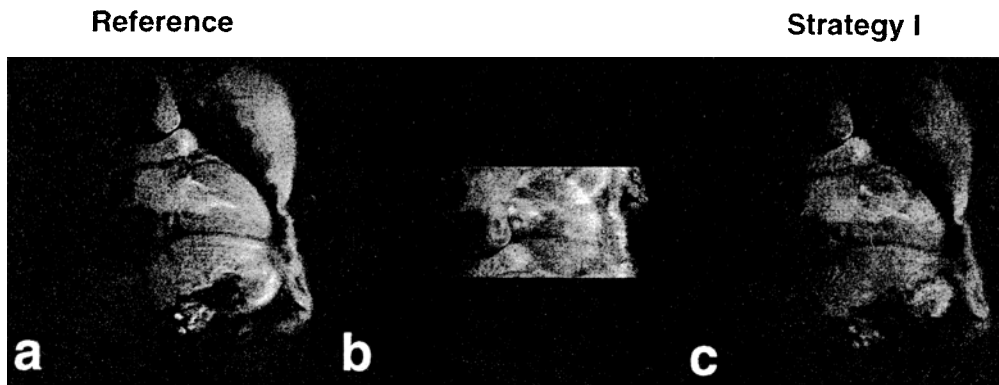
Reference   **Strategy I**

Fig. 7. Results obtained from a cardiac study with strategy I using three spatial harmonics. (a) Reference image (240 × 256 matrix size) obtained in 48 cardiac cycles corresponding to a breath-hold time of 40 s. (b) Aliased image (80 × 256 matrix size) obtained in 16 cardiac cycles with reduced gradient phase encoding. This image was formed by combining the component coil reference images pixel-by-pixel as the square root of the sum of square magnitudes. (c) The corresponding full FOV image after AUTO-SMASH reconstruction (240 × 256 matrix size). Acquisition time of this image was 16 cardiac cycles or 1/3 of the reference acquisition time.

and therefore SMASH and other PPA image reconstructions difficult. AUTO-SMASH allows for more flexible and more convenient acquisition and postprocessing procedures.

6. Conclusion

We have developed an internal sensitivity calibration technique for the SMASH imaging method using additionally acquired self-calibration signals. This procedure acquires the necessary coil sensitivity information in the course of the actual scan, rather than in a separate calibration experiment. The advantage of this sensitivity reference method is that no extra coil array sensitivity maps need to be acquired. In addition, AUTO-SMASH provides coil sensitivity information in areas of non-uniform spin-density and moving tissue structures, where no reliable direct coil sensitivity measurements are possible. Data post-processing is easy to implement and the underlying concept can be combined easily with most conventional or fast imaging techniques. The results from the self-calibrating SMASH approach in phantoms and human subjects indicate that this technique is an effective method for internal calibration of SMASH images. Since parallel imaging techniques have the potential to play an important role in the area of fast MR imaging, the need for a fast and accurate coil sensitivity calibration will likely increase. Therefore the approach of using additionally sampled calibration signals, as demonstrated with AUTO-SMASH, may play an im-

portant role for rapid parallel imaging techniques in times to come.

References

[1] Hutchinson M, Raff U. Fast MRI data acquisition using multiple detectors. Magn Reson Med 1988;6:87–91.

[2] Kwiat D, Einav S, Navon G. A decoupled coil detector array for fast image acquisition in magnetic resonance imaging. Med Phys 1991;18:251–65.

[3] Carlson JW, Minemura T. Imaging time reduction through multiple receiver coil data acquisition and image reconstruction. Magn Reson Med 1993;29:681–8.

[4] Kelton JR, Magin RL, Wright SM. An Algorithm For Rapid Image Acquisition Using Multiple Receiver Coils, in: Proc., SMRM, 8th Annual Meeting, 1989, p. 1172.

[5] Ra JB, Rim CY. Fast imaging using subencoding data sets from multiple detectors. Magn Reson Med 1993;30:142–5.

[6] Sodickson DK, Manning WJ. Simultaneous acquisition of spatial harmonics (SMASH): Fast imaging with radiofrequency coil arrays. Magn Reson Med 1997;38:591–603.

[7] Sodickson DK, Bankson JA, Griswold MA, Wright SM. Eightfold improvements in MR Imaging speed using SMASH with a multiplexed eight-element array. Proc 6th Sci Meeting Int Soc Magn Res Med, 1998, p. 577.

[8] Axel L, Constantini J, Listerud J. Intensity correction in surface-coil MR imaging. AJR 1987;148:418–20.

[9] Murakami JW, Hayes CE, Weinberger E. Intensity correction of phase array surface coil images. Magn Reson Med 1996;35:585–90.

[10] Sodickson DK, Griswold MA, Jakob PM, Edelman RR, Manning WJ. Signal-to-noise ratio and signal-to-noise efficiency in SMASH imaging. Proc. 6th Sci Meeting Int Soc Magn Res Med, 1998, p. 1957.

[11] Sodickson DK, Griswold MA, Jakob PM, Edelman RR, Manning WJ (1998) Signal-to-noise ratio and signal-to-noise efficiency in SMASH imaging. Magn Reson Med (Submitted for publication).